Proc. Natl. Acad. Sci. USA
Vol. 83, pp. 503–507, January 1986
Neurobiology

X-ray diffraction from intraneuronal paired helical filaments and extraneuronal amyloid fibers in Alzheimer disease indicates cross-β conformation

(aging/fibrous proteins/protein conformation/amyloidosis)

DANIEL A. KIRSCHNER*†, CARMELA ABRAHAM*‡, AND DENNIS J. SELKOE*‡

*Departments of Neuropathology and Neurology, Harvard Medical School, Boston, MA 02115; †Department of Neuroscience, Children's Hospital, Boston, MA 02115; and ‡Center for Neurologic Diseases, Brigham and Women's Hospital, Boston, MA 02115

Communicated by Francis O. Schmitt, September 18, 1985

ABSTRACT **Information about the structure of the paired helical filaments (PHF) that accumulate within human neurons and the amyloid fibers that accumulate in the extracellular spaces between neurons in Alzheimer disease has so far depended on electron microscopy of thin-sectioned or negatively stained material. To determine the protein conformation of these abnormal fibers, we have obtained x-ray diffraction patterns from unfixed human brain fractions highly enriched in PHF and from purified amyloid cores isolated from senile plaques. The predominant x-ray scatter evident from both types of samples, either wet or dry, is a sharp reflection at 4.76-Å spacing and a diffuse one at about 10.6-Å spacing. These features are characteristic of a β-pleated sheet type of protein conformation. In doubly oriented dried pellets of PHF fractions, the two reflections are accentuated at right angles to each other and the arc at 4.76-Å spacing is in the fiber direction indicating a cross-β conformation. From the integral widths of the reflections we estimate the cross-β crystallite to be about 80 Å long in the fiber direction and about 40 Å thick. These dimensions correspond to approximately four pleated sheets, each of which consists of approximately 16 hydrogen-bonded polypeptide chains running normal to the fiber direction. The cross-β conformation of PHF and amyloid fibers that we have found from x-ray diffraction is in contrast to the predominant α-helical coiled-coil conformation of the neurofilaments with which they share epitopes and from which they have been postulated to derive.**

Protein-rich tissue deposits that exhibit a green birefringence after Congo red staining and are fibrous in appearance in the electron microscope are classified as amyloid (1, 2). X-ray diffraction of amyloid isolated from humans with primary and secondary systemic amyloidoses reveals that the major proteinaceous component has a cross-β pleated sheet conformation (3, 4). In Alzheimer disease, pathological accumulations of congophilic fibrous material occur as neurofibrillary tangles within neuronal cell bodies, in neuritic (or senile) plaques, and in the walls of certain cerebral blood vessels (5). Qualitatively indistinguishable amyloid deposits also occur in normal aged human brains but in much smaller numbers and in restricted topographical distribution.

Electron microscopy reveals that the major organized structural components of neurofibrillary tangles are 160–220 Å (diameter) paired helical filaments (PHF) that narrow to 60–100 Å in diameter about every 800 Å (6–8). Such fibers are also observed in the dystrophic neurites that comprise the senile plaques. In addition, extracellular amyloid composed of 40–90 Å (diameter) fibrils form the central cores of senile plaques (9, 10). Structurally similar filaments are observed in some meningeal and intracerebral blood vessels (11–13).

The optical properties of amyloid as revealed by Congo red staining have been shown to depend on the β-pleated sheet conformation of protein (14). Therefore, the Congo red birefringence of PHF would suggest a similar conformation for this fibrous protein. The filamentous shape and dimensions of PHF, however, suggest a similarity to and possible derivation from intermediate filaments such as neurofilaments, which are prominent cytoskeletal elements in neurons. The major proteins of intermediate filaments have been shown to have primarily a coiled-coil α-helical conformation (15–17), although they may contain small β-pleated sheet domains (16, 17).

To determine directly the protein conformation in PHF, we have undertaken an x-ray diffraction study of highly enriched PHF fractions from Alzheimer disease brain tissue. We have also examined purified amyloid cores isolated from Alzheimer-type senile plaques. The spacings measured from x-ray patterns of these fibers should provide evidence for an α, β, or cross-β conformation (18). A preliminary report of this work has been presented (19).

MATERIALS AND METHODS

Purification of PHF and of Amyloid Cores. PHF were purified from frozen cerebral cortex of Alzheimer patients (20). Pellets for x-ray diffraction were taken from the 1.4/2.0 M sucrose gradient interface and repelleted in 0.1% or 0.05% $NaDodSO_4$ into hemi-hyperboloid Beem capsules. The supernatant was then replaced with distilled water, and the wet pellet was sealed in a thin-wall glass capillary for x-ray diffraction.

Senile plaque amyloid cores were obtained as crude isolates in the low-speed pellets of cerebral cortical homogenates and were further purified by a new method employing fluorescence-activated particle sorting (21). Concentrated, highly purified pellets of amyloid cores in 0.1% $NaDodSO_4$ were resuspended, injected into glass x-ray capillaries by using a Hamilton syringe, and gently spun down in a clinical centrifuge ($200 \times g$, 5 min). The $NaDodSO_4$ supernatant was replaced with distilled water, and the pellet was then examined by x-ray diffraction.

Microscopy. Small samples were removed from the PHF and amyloid core pellets and examined between crossed polarizers in the light microscope after staining with Congo red and in the electron microscope after fixing with 2.5% buffered glutaraldehyde.

X-ray Diffraction. The x-ray diffraction measurements were made by using nickel-filtered and double-mirror focused CuK_α radiation from a fine-line source on a Rigaku generator operated at 40 kV, 20 mA. The patterns were recorded on Kodak direct-exposure x-ray film during exposure times of

The publication costs of this article were defrayed in part by page charge payment. This article must therefore be hereby marked "*advertisement*" in accordance with 18 U.S.C. §1734 solely to indicate this fact.

Abbreviation: PHF, paired helical filament(s).

several days to 1 week. The specimen to film distance was 68.5 mm, which was determined by recording the diffraction from known standards (NaCl, calcite, and cholesterol). The spacings of the diffraction spectra were measured directly off the x-ray films viewed at 6× magnification or measured from the densitometer scans of the films. The optical densities of the films were determined on an Optronics Photoscan P-1000 microdensitometer (using a 50-μm raster) controlled by a DEC VAX 11/780 computer. To maximize the signal-to-background in the densitometer scans of our films, we used a computer program that enabled us to integrate the optical densities along arcs with respect to the center of the pattern and within a defined angle. Integral widths of the reflections were calculated by dividing their peak areas above background by their peak heights and correcting for the finite width of the x-ray beam, which was <300 μm square. The corrected integral widths are inversely related to the size of the diffracting regions or coherence lengths (22). The precision of individual integral width measurements on the relatively sharp reflection at 4.76 Å was about 10%, whereas that on the broad reflection at 10.6 Å was about 20%. These uncertainties directly reflect the signal-to-noise level for each peak.

RESULTS

Purity of Samples. Birefringent Congo red-stained assemblies were observed by polarization microscopy in the samples from the PHF and amyloid core pellets, confirming the high degree of enrichment of the isolates. Electron microscopy indicated that the PHF pellets (Fig. 1*a*) consisted of masses of PHF in various-sized aggregates, electron-dense lipofuscin granules, and occasional membranous profiles. The purified amyloid core pellets (Fig. 1 *b* and *c*) were virtually free of any contaminating material and consisted of >90% amyloid cores by both light and electron microscopic particle counts. The remaining particles were small aggregates of lipofuscin granules.

To control for the contaminating presence of lipofuscin and the $NaDodSO_4$ that might remain after purification, we recorded x-ray patterns from lipofuscin-rich fractions of aged human cerebral cortex (isolated in buffers containing $NaDodSO_4$) and from pure $NaDodSO_4$. The lipofuscin was characterized by very strong small-angle scatter centered at approximately 60-Å spacing and weak wide-angle reflections around 4.2- and 4.8-Å spacings. The pure $NaDodSO_4$ as well as PHF pellets from which excess $NaDodSO_4$ had not been washed out gave a series of sharp, small-angle reflections

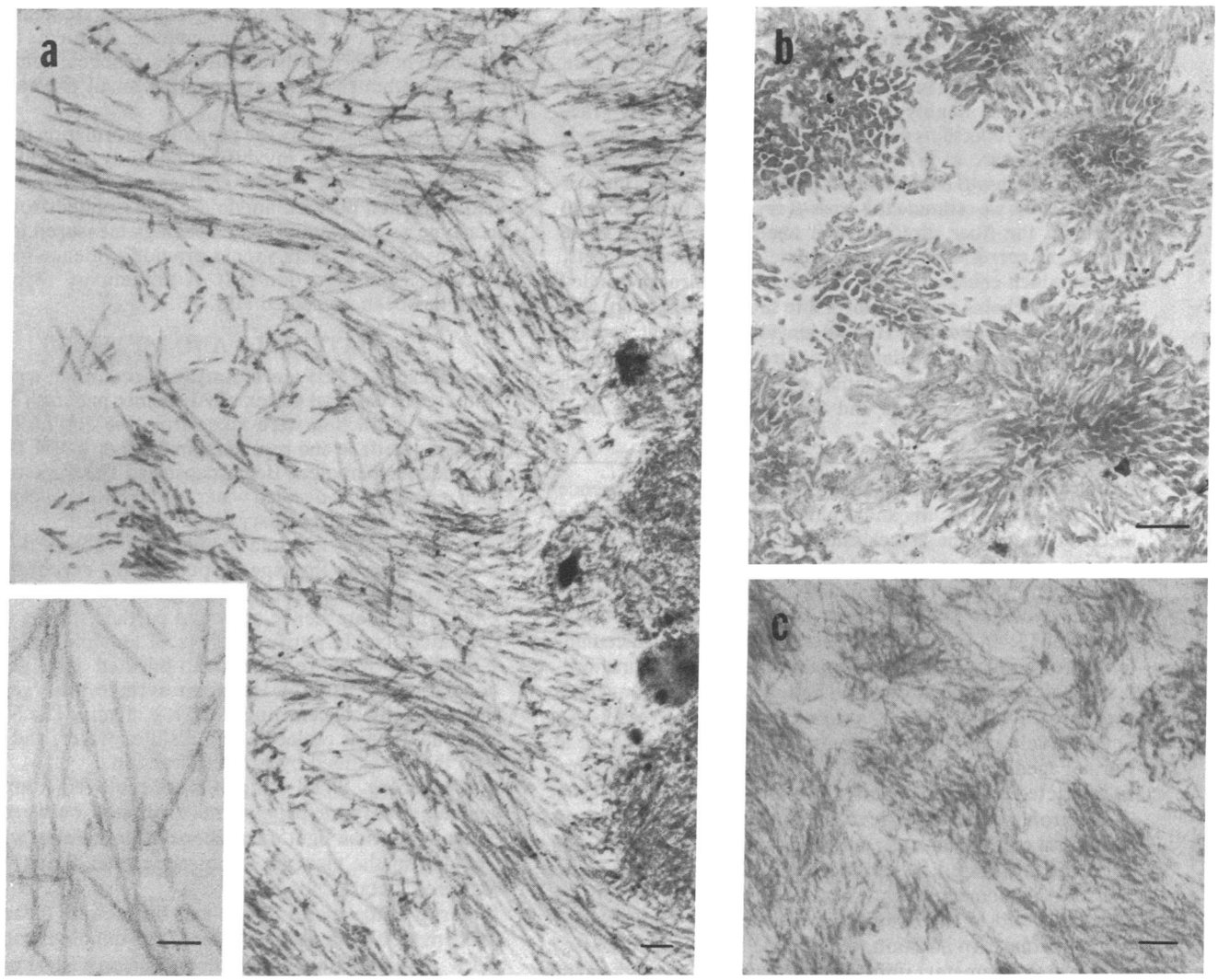

FIG. 1. Electron micrographs of fiber preparations. (*a*) A highly enriched fraction of PHF from Alzheimer cerebral cortex prepared as described (20). (Bar = 1000 Å.) (*Inset*) Higher magnification of PHF. (Bar = 1000 Å.) (*b*) Low-magnification view of purified amyloid cores prepared by differential and sucrose gradient centrifugation and fluorescence-activated particle sorting (21). (Bar = 2 μm.) (*c*) Higher magnification of amyloid filaments comprising the cores. (Bar = 1000 Å.)

with a repeat of about 39 Å and some wide-angle reflections between 4.1 and 4.4 Å.

X-ray Diffraction from PHF Pellets. X-ray patterns from a PHF pellet at different hydrations showed reflections that were distinguishable from those of lipofuscin and $NaDodSO_4$. As the pellet dried, the diffuse water ring at 3.3-Å spacing became progressively weaker, and a sharp ring at about 4.76-Å spacing as well as a broad ring at about 10.6-Å spacing became stronger (Figs. 2 and 3, traces a–c). The same results were obtained with PHF pellets prepared from three different Alzheimer brains, including one with the familial (autosomal dominant) form of the disease.

Electron microscopy of our pellets indicated that the fiber axes of the individual filaments lie randomly in the plane of the pellet—i.e., perpendicular to the direction of centrifugation. When the pellets were aligned with their edges toward the x-ray beam (i.e., perpendicular to the direction of centrifugation) the 4.76-Å spacing occurred as arcs in a direction parallel to the plane of the pellets. When the pellet was aligned with its face toward the x-ray beam, the 4.76-Å spacing was a ring. In contrast, the 10.6-Å spacing was recorded as a ring for both orientations of the pellets. Therefore, the 4.76-Å spacing comes from a periodicity along the fiber axes of the filaments, whereas the 10.6-Å spacing comes from a periodicity perpendicular to the fiber axis.

These x-ray spacings are characteristic of a β-pleated sheet conformation in which 4.76 Å corresponds to the spacing between neighboring hydrogen-bonded polypeptide chains, and 10.6 Å corresponds to the distance between the pleated sheets. The patterns from the singly oriented centrifugation pellets suggested that the β-pleated sheet was of the cross-β type, with the hydrogen-bonding direction along the fiber axis.

X-Ray Diffraction from Partially Oriented PHF Pellets. To determine more definitively the type of β conformation, we examined a pellet that upon slow dehydration over saturated KCl and then over $CaCl_2$ had become partially oriented along the wall of the capillary. When the x-ray beam was directed perpendicular to the capillary wall, the reflections at 4.76-Å and about 10.6-Å spacings appeared as arcs that were accentuated at right angles to each other (Figs. 2 and 3, traces b and c). This demonstrates a cross-β conformation in which the polypeptide chains or β strands lie in a direction at right angles to the fiber axis (18). The accentuation of the 4.76-Å arcs along the capillary axis indicated that the PHF fibers were predominantly oriented parallel to the capillary axis. We next removed the partially oriented pellet from the capillary and reinserted it so that the x-ray beam could be directed parallel to the fiber axis. In this geometry, the intensity of the approximately 10.6-Å intersheet spacing was enhanced relative to that of the 4.76-Å spacing.

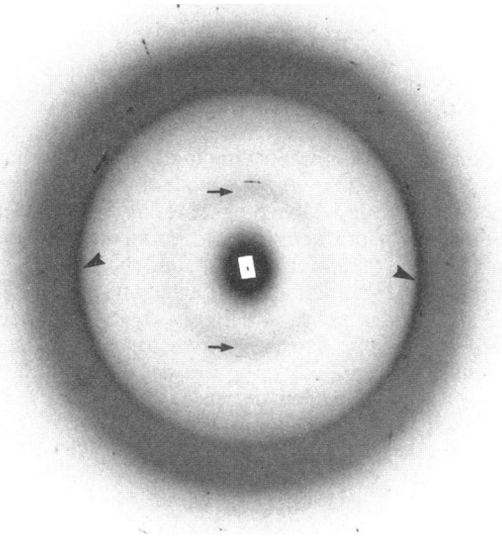

FIG. 2. X-ray diffraction pattern from a partially oriented, dried PHF pellet. The beam was directed normal to the fiber axis, which is vertical. The meridionally accentuated arcs at 4.76-Å spacing are indicated by the arrowheads, and the equatorially accentuated arcs centered at about 10.6-Å spacing are indicated by the arrows.

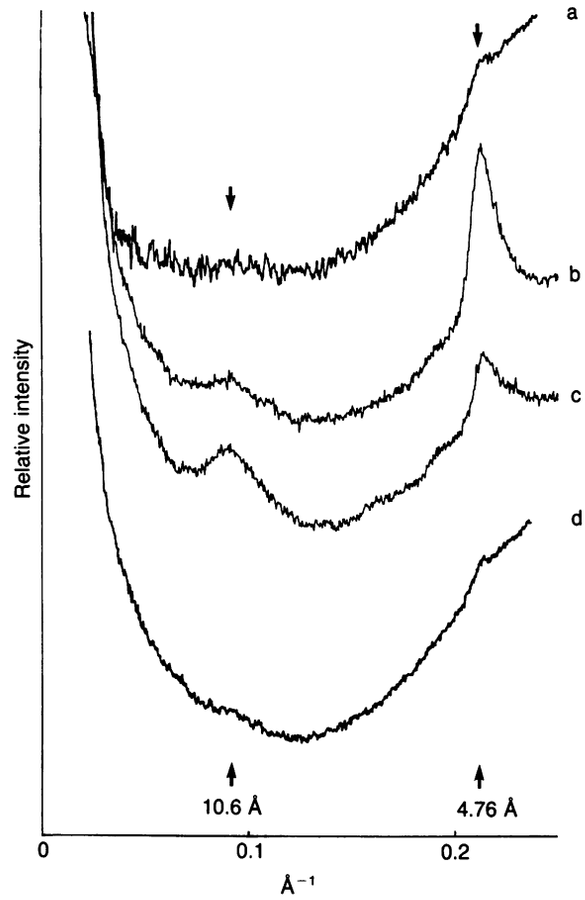

FIG. 3. Densitometer scans of x-ray patterns from intraneuronal PHF and extraneuronal amyloid pellets. Trace a, wet centrifuge pellet of PHF. Traces b and c, meridional (trace b) and equatorial (trace c) scans of dry, partially oriented PHF pellet. Trace d, dry pellet of amyloid. The positions of the approximately 10.6-Å intersheet and 4.76-Å interchain spacings are indicated. The scans have been offset in the vertical direction for clarity. Note in traces b and c how the interchain spacing is accentuated along the meridian, whereas the intersheet spacing is accentuated along the equator.

X-ray Diffraction from Amyloid Cores. Purified pellets of amyloid cores gave x-ray diffraction patterns indicating a β conformation for the protein. The sharp 4.76-Å spacing as well as a broad intensity maximum in the 10- to 11-Å region were observed in the wet pellet and after partial drying (Fig. 3, trace d). These reflections remained as unoriented rings, even after gradual drying.

Dimensions of the Cross-β Crystallite of PHF. We estimated the coherence length or size of the diffracting region from the integral widths of the reflections at 4.76- and 10.6-Å spacings. Five measurements on the 4.76-Å reflection from three different PHF samples gave a mean value (±SD) of 76 ± 11 Å for the length of the crystallite (in the fiber direction). This length corresponds to 16 ± 2 polypeptide chains (β strands) hydrogen-bonded to one another within the pleated sheet. Only two of the PHF samples gave x-ray scatter at 10.6 Å that was satisfactory for quantitation from the densitometer

scans. Three measurements on this reflection from these samples gave a mean value (±SD) of 42 ± 2 Å for the thickness of the stack of pleated sheets. This thickness corresponds to four sheets. Fig. 4 summarizes the dimensions of the cross-β crystallite for PHF according to our x-ray diffraction measurements.

DISCUSSION

Our study demonstrates that the PHF of human neurofibrillary tangles is principally organized at the molecular level in a cross-β pleated sheet conformation. Amyloid purified from senile plaques in human brain also has this conformation, based on the similarity of the x-ray patterns from unoriented pellets of amyloid and PHF. The x-ray spacings at 4.76 Å and 10.6 Å were typical of the PHF and amyloid pellets examined and were distinguished from the scatter from any residual $NaDodSO_4$ or contaminating lipofuscin. It is unlikely that the use of $NaDodSO_4$ in the purifications resulted in any appreciable conformational alterations in the proteins since the purified material retained both the Congo red birefringence as well as the electron microscopic ultrastructure characteristic of the starting tissues. Furthermore, $NaDodSO_4$-isolated PHF and senile plaque cores still bind specific antibodies that label these fibers in their native state in tissue sections (20, 21).

In thin sections, PHF appear to be composed of two approximately 100-Å (diameter) filaments that are helically wound with a pitch of approximately 800 Å (6–8). An electron-lucent region along the axis of the structure supports this model. Negatively stained PHF, however, do not show a prominent line of stain along the axis, as would be expected for such a model; rather, four 30- to 50-Å (diameter) protofilaments have been reported (23, 24). In addition, ultrathin cross sections of PHF suggest the presence of eight protofilaments (25).

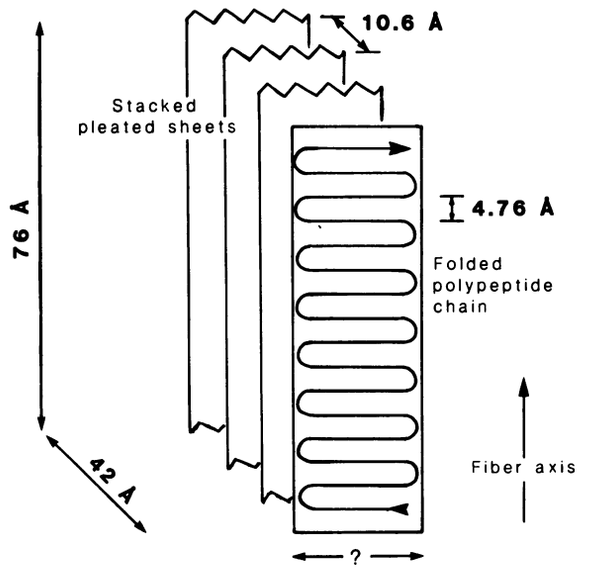

FIG. 4. Schematic diagram summarizing our analysis of the x-ray diffraction patterns from PHF and indicating the dimensions deduced for the cross-β crystallite constituting PHF. The polypeptide chain is shown in an anti-parallel configuration, like that for all known examples of synthetic polypeptides and fibrous proteins that have a β conformation. The β-strand length (indicated by the ?) has not yet been determined by the x-ray diffraction analysis; however, it may be 30–50 Å based on the estimated diameter of the protofilament observed in the electron microscope. To account for the dimensions of thin-sectioned and negatively stained PHF, a crystallite would correspond to the structural unit of the protofilaments that are assembled to form PHF.

Correlation of our x-ray diffraction measurements with the electron microscopic observations suggest that the underlying structural unit of the protofilament is a cross-β crystallite that is 76 Å long and 42 Å thick, with four β-pleated sheets constituting this thickness. Axially, about 10 crystallites arrayed end-to-end could account for the pitch of the PHF helix. Transversely, the crystallites could pack either face-to-face or side-to-side in two rows to give the minimum (60–100 Å) and maximum (160–220 Å) diameters observed in the electron microscope. Assuming that the width of the β-pleated sheet is similar to the 30- to 50-Å diameter of the negatively stained protofilament, we estimate that 10–15 amino acid residues comprise each β strand.

The ultrastructural dimensions of other cross-β fibrous proteins have been deduced from x-ray diffraction, electron diffraction, or secondary structure analysis. The length of the β strands is eight residues in *Chrysopa* silk (26) and in the distal half of the tail fiber of bacteriophage T4 (27) and averages about the same in the narrow shaft of the adenovirus fiber protein (28). This is slightly less than the lowest estimate for the β-strand length in PHF. In the bacteriophage and in the adenovirus a dimer of cross-β pleated sheets constitutes the fibers, whereas in *Chrysopa* a variable number of cross-β pleated sheets packs together to form the fiber. The thickness of the β crystallite in PHF, in comparison, appears to be determined by a stack of about four pleated sheets.

The cross-β conformation of PHF and brain amyloid may be surprising in view of the fact that epitopes of neurofilaments, which are primarily α proteins, have been found either closely associated with or in PHF and amyloid fibers (29–34). Further, a recent electron microscope study shows apparent continuity of neurofilaments with PHF (35). When analyzed for secondary structure, the 68-kDa neurofilament protein shows β domains in the 7-kDa amino-terminal headpiece and also in the proximal 5-kDa segment of the carboxyl-terminal tailpiece (16). The amino-terminal headpiece of the 160-kDa neurofilament protein also has been reported to include an approximately 7-kDa β domain (16). If PHF are derived from intermediate filaments, then perhaps the preexisting β domains become predominant and aggregate or polymerize as the α-helical domains are disarrayed or degraded. A similar pathogenetic mechanism may also underlie the formation of amyloid in organ-limited cutaneous amyloidosis, a disorder in which the α-keratin filaments in degenerating keratinocytes appear to accumulate as deposits of Congo red birefringent amyloid (36, 37).

The high degree of insolubility of PHF and amyloid core fibers in detergents, chaotropic salts, and weak acids (21, 38–42) presumably derives from the extensive regular array of intramolecular hydrogen bonding and also perhaps from nonpolar interactions and/or covalent bonds between the β-pleated sheets. It has been observed recently that sequential treatment of purified amyloid cores with concentrated (approximately 80%) formic acid and $NaDodSO_4$ or with saturated (6.8 M) guanidine thiocyanate and $NaDodSO_4$ leads to the disappearance of the fibers by light and electron microscopy and the release of two low molecular weight polypeptides that appear to be dimerically related (21, 42). Similar proteins can also be released from PHF-enriched fractions by these reagents; however, whether the proteins actually derive from the PHF per se is not yet established. Those portions of the fibers that are solubilized by such treatment are presumably stabilized by multiple, strong noncovalent interactions—e.g., the hydrogen bonding of the cross-β conformation reported here—without the need to hypothesize covalent crosslinks (43). The possibility that certain portions of the fibers are stabilized by crosslinks, however, cannot yet be excluded.

Previous x-ray diffraction studies on amyloid from liver and spleen of humans or animals with amyloidosis (3, 4)

reveal a cross-β structure for the filamentous protein. The 4.76-Å interchain spacing is like that for the intracellular PHF and extracellular amyloid core fibers of human central nervous system; however, the 9.8-Å intersheet spacing for the systemic amyloid is nearly 1 Å less than that for the central nervous system amyloids. Since the composition of the amino acid residues determines the packing of the pleated sheets, then the side chains must differ between the systemic and neuronal amyloids. In contrast to virtually all amyloid proteins observed previously, the PHF that accumulate in aging human brain and particularly in Alzheimer disease are found intracellularly. The initial stimulus that causes the neuron to form such highly inert fibers in its cytoplasm and leads to the deposition of amyloid fibers in the extraneuronal space remains unknown.

We thank Drs. Hideyo Inouye and Laszlo Lorand for useful discussions, William M. Hamilton for electron microscopy, Gary Weil and Christopher Smith for assistance in the amyloid core purifications, Josh Simons for the densitometry program, and William P. McIntosh for photographic services. The research was supported by National Institutes of Health Grants NS 20824 (D.A.K.), AG 01307 (D.J.S.), and NS 20110 (D.J.S.). The work was carried out in facilities related to the Mental Retardation Research Center at Children's Hospital, Inc., and was supported by National Institutes of Health Core Grant HD 06276.

1. Glenner, G. G. (1980) *New Engl. J. Med.* **302,** 1283–1292.
2. Cohen, A. S., Shirahama, T. & Skinner, M. (1982) in *Electron Microscopy of Proteins*, ed. Harris, J. R. (Academic, London), pp. 165–205.
3. Eanes, E. D. & Glenner, G. G. (1968) *J. Histochem. Cytochem.* **16,** 673–677.
4. Bonar, L., Cohen, A. S. & Skinner, M. M. (1969) *Proc. Exp. Biol. Med.* **131,** 1373–1375.
5. Tomlinson, B. E. & Corsellis, J. A. N. (1984) in *Greenfield's Neuropathology*, eds. Adams, J. H., Corsellis, J. A. N. & Duchen, L. W. (Arnold, London), 4th Ed., pp. 951–980.
6. Kidd, M. (1963) *Nature (London)* **197,** 192–193.
7. Terry, R. D. (1963) *J. Neuropathol. Exp. Neurol.* **22,** 629–642.
8. Wisniewski, H. M., Narang, H. K. & Terry, R. D. (1976) *J. Neurol. Sci.* **27,** 173–181.
9. Narang, H. K. (1980) *J. Neuropathol. Exp. Neurol.* **39,** 621–631.
10. Merz, P. A., Wisniewski, H. M., Somerville, R. A., Bobin, S. A., Master, C. L. & Iqbal, K. (1983) *Acta Neuropathol.* **60,** 113–124.
11. Vanley, C. T., Arguilar, M. J., Kleinhenz, R. J. & Lagois, M. D. (1981) *Hum. Pathol.* **12,** 609–616.
12. Glenner, G. G. (1983) in *Biological Aspects of Alzheimer's Disease*, Banbury Report, ed. Katzman, R. (Cold Spring Harbor Laboratory, Cold Spring Harbor, NY), Vol. 15, pp. 137–144.
13. Glenner, G. G. & Wong, C. W. (1984) *Biochem. Biophys. Res. Commun.* **120,** 883–890.
14. Glenner, G. G., Eanes, E. D. & Page, D. L. (1972) *J. Histochem. Cytochem.* **20,** 821–826.
15. Crewther, W. G., Dowling, L. M., Steinert, P. M. & Parry, D. A. D. (1983) *Int. J. Macromol.* **5,** 267–274.
16. Geisler, N., Kaufmann, E., Fischer, S., Plessmann, U. & Weber, K. (1983) *EMBO J.* **2,** 1295–1302.
17. Wais-Steider, C., Eagles, P. A. M., Gilbert, D. S. & Hopkins, J. M. (1983) *J. Mol. Biol.* **165,** 393–400.
18. Fraser, R. D. B. & MacRae, T. P. (1973) *Conformation in Fibrous Proteins and Related Synthetic Polypeptides* (Academic, New York), pp. 179–246.
19. Kirschner, D. A., Abraham, C. & Selkoe, D. J. (1985) *Trans. Am. Soc. Neurochem.* **16,** 142 (abstr.).
20. Ihara, Y., Abraham, C. R. & Selkoe, D. J. (1983) *Nature (London)* **304,** 727–730.
21. Selkoe, D. J., Abraham, C. R. & Duffy, L. K. (1986) *J. Neurochem.*, in press.
22. Alexander, L. E. (1979) *X-Ray Diffraction Methods in Polymer Science* (Krieger, New York), p. 423f.
23. Wisniewski, H. M., Merz, P. A. & Iqbal, K. (1984) *J. Neuropathol. Exp. Neurol.* **43,** 643–656.
24. Crowther, R. A., Wischik, C. M. & Stewart, M. (1985) in *Proceedings of the 43rd Annual Meeting of the Electron Microscopy Society of America*, ed. Bailey, G. W. (San Francisco Press, San Francisco), pp. 734–737.
25. Wisniewski, H. M. & Wen, G. Y. (1984) in *International Conference on Intermediate Filaments* (N.Y. Acad. Sci., New York), p. 48.
26. Geddes, A. J., Parker, K. D., Atkins, E. D. T. & Beighton, E. (1968) *J. Mol. Biol.* **32,** 343–358.
27. Earnshaw, W. C., Goldberg, E. B. & Crowthers, R. A. (1979) *J. Mol. Biol.* **132,** 101–131.
28. Green, N. M., Wrigley, N. G., Russell, W. C., Martin, S. R. & McLachlan, A. D. (1983) *EMBO J.* **2,** 1357–1365.
29. Gambetti, P., Velasco, M. E., Dahl, D., Bignami, A., Roessmann, U. & Sindely, S. D. (1980) in *Aging of the Brain and Dementia*, eds. Amaducci, L., Davison, A. N. & Antuono, P. (Raven, New York), pp. 55–63.
30. Ihara, Y., Nukina, N., Sugita, H. & Toyokura, Y. (1981) *Proc. Jpn. Acad.* **57,** 152–156.
31. Powers, J. M., Schlaepfer, W. W., Wellingham, M. C. & Hall, B. J. (1981) *J. Neuropathol. Exp. Neurol.* **40,** 592–612.
32. Anderton, B. H., Breinburg, D., Downes, M. J., Green, P. J., Tomlinson, B. E., Ulrich, J., Wood, J. N. & Kahn, J. (1982) *Nature (London)* **298,** 84–86.
33. Autilio-Gambetti, L., Gambetti, P. & Crane, R. C. (1983) in *Biological Aspects of Alzheimer's Disease*, Banbury Report, ed. Katzman, R. (Cold Spring Harbor Laboratory, Cold Spring Harbor, NY), Vol. 15, pp. 117–124.
34. Rasool, C. G., Abraham, C., Anderton, B. H., Hough, M., Kahn, J. & Selkoe, D. J. (1984) *Brain Res.* **310,** 249–260.
35. Yoshimura, N. (1984) *Clin. Neuropathol.* **3,** 22–27.
36. Kumakiri, M. & Hashimoto, K. (1979) *J. Invest. Dermatol.* **73,** 150–162.
37. Hashimoto, K. & Kobayashi, H. (1980) *Am. J. Dermatopathol.* **2,** 165–171.
38. Selkoe, D. J., Ihara, Y. & Salazar, F. J. (1982) *Science* **215,** 1243–1245.
39. Selkoe, D. J., Ihara, Y., Abraham, C., Rasool, C. G. & McCluskey, A. H. (1983) in *Biological Aspects of Alzheimer's Disease*, Banbury Report, ed. Katzman, R. (Cold Spring Harbor Laboratory, Cold Spring Harbor, NY), Vol. 15, pp. 125–134.
40. Yen, S. H. & Kress, Y. (1983) in *Biological Aspects of Alzheimer's Disease*, Banbury Report, ed. Katzman, R. (Cold Spring Harbor Laboratory, Cold Spring Harbor, NY), Vol. 15, pp. 155–165.
41. Goni, F., Pons-Estel, B., Alvarez, F., Gorevic, P. & Frangione, B. (1985) *Proceedings of the 4th International Symposium on Amyloidosis*, ed. Glenner, G. G. (Plenum, New York), in press.
42. Masters, C. L., Simms, G., Weinman, N. A., Multhaup, G., McDonald, B. L. & Beyreuther, K. (1985) *Proc. Natl. Acad. Sci. USA* **82,** 4245–4249.
43. Selkoe, D. J., Abraham, C. & Ihara, Y. (1982) *Proc. Natl. Acad. Sci. USA* **79,** 6070–6074.